J Neurophysiol 120: 1307–1317, 2018.
First published May 18, 2018; doi:10.1152/jn.00234.2018.

RESEARCH ARTICLE | *Neural Circuits*

Minocycline promotes posthemorrhagic neurogenesis via M2 microglia polarization via upregulation of the TrkB/BDNF pathway in rats

Hongsheng Miao,[1] Runming Li,[2] Cong Han,[1] Xiuzhen Lu,[1] and Hang Zhang[2]
[1]*Department of Neurosurgery, Shanghai General Hospital, Shanghai Jiaotong University School of Medicine; and*
[2]*Department of Neurosurgery, No. 205 Hospital of People's Liberation Army of China, Jingzhou, China*

Submitted 5 April 2018; accepted in final form 16 May 2018

Miao H, Li R, Han C, Lu X, Zhang H. Minocycline promotes posthemorrhagic neurogenesis via M2 microglia polarization via upregulation of the TrkB/BDNF pathway in rats. *J Neurophysiol* 120: 1307–1317, 2018. First published May 18, 2018; doi:10.1152/jn.00234.2018.—Intracerebral hemorrhage (ICH) is a devastating disease worldwide with increasing mortality. The present study investigated whether minocycline was neuroprotective and induced M2 microglial polarization via upregulation of the TrkB/BDNF pathway after ICH. ICH was induced via injection of autologous blood into 150 Sprague-Dawley rats. A selective TrkB antagonist [N2–2-2-oxoazepan-3-yl amino] carbonyl phenyl benzo (b) thiophene-2-carboxamide (ANA 12)] and agonist [*N*-[2-(5-hydroxy-1H-indol-3-yl) ethyl]-2-oxopiperidine-3-carboxamide (HIOC)] were used to investigate the mechanism of minocycline-induced neuroprotection. Minocycline improved ICH-induced neurological deficits and reduced M1 microglia marker protein (CD68, CD16) expression as well as M2 microglial polarization (CD206 and arginase 1 protein). Minocycline administration enhanced microglia-neuron cross talk and promoted the proliferation of neuronal progenitor cells, such as DCX- and Tuj-1-positive cells, 24 h after ICH. Minocycline also increased M2 microglia-derived brain-derived neurotrophic factors (BDNF) and the upstream TrkB pathway. ANA 12 reversed the neuroprotective effects of minocycline. HIOC exhibited the same effects as minocycline and accelerated neurogenesis after ICH. This study demonstrated for the first time that minocycline promoted M2 microglia polarization via upregulation of the TrkB/BDNF pathway and promoted neurogenesis after ICH. This study contributes to our understanding of the therapeutic potential of minocycline in ICH.

NEW & NOTEWORTHY The present study gives several novel points: *1*) Minocycline promotes neurogenesis after intracerebral hemorrhage in rats. *2*) Minocycline induces activated M1 microglia into M2 neurotrophic phenotype. *3*) M2 microglia secreting BDNF remodel the damaged neurocircuit.

ICH; microglial polarization; minocycline; neurogenesis; TrkB/BDNF pathway

INTRODUCTION

Intracerebral hemorrhage (ICH) remains an urgent medical-social problem that accounts for almost 15% of stroke occurrence (Lei et al. 2015). The world is facing an ICH epidemic with declining mortality rates, which means that more survivors with serious disabilities are waiting for effective medical cure (Hankey 2017; Hemphill et al. 2015). Microglia activation plays a key role in the process of ICH pathology (Chen et al. 2015; Li et al. 2015). Increasing positive functions of microglia are reported, such as neurogenesis and synapse formation, despite the role of these cells in inflammation (Gemma and Bachstetter 2013; Kim et al. 2013).

Microglia are resident macrophages in the brain, and these cells are the first responders of the immune system (Zhao et al. 2015). Microglia are generally classified into M1- and M2-polarized states, but they can continually move between these two extreme states (Hu et al. 2015). Studies suggest the classification of polarized microglia into an activation state between a neuro-harmful and protective state (Kobayashi et al. 2013), which avoids the oversimplification. M1 microglia express proinflammatory factors, such as tumor necrosis factor α (TNF-α) and interleukin-1β (IL-1β), and surface markers, such as CD68 and CD16 (Lan et al. 2017; Pan et al. 2015). CD206, arginase 1, and IL-10 are special expression factors in M2 microglia (Kigerl et al. 2009; Ponomarev et al. 2007; Quirié et al. 2013). Recent research on microglia polarization opened a new window in the search for therapeutic targets following brain injury, such as hemorrhagic stroke, ischemia stroke, and traumatic brain injury (Kumar et al. 2016; Perego et al. 2016; Wan et al. 2016). However, most of the current reagents are pathway agonists or antagonists, and few of these drugs are used clinically.

Minocycline is a semisynthetic second-generation derivative of tetracycline and is widely used to reduce bacterial burden and inflammation (Daly et al. 2016). Minocycline is highly lipophilic and easily penetrates the brain-blood barrier (BBB) (Zhao et al. 2011). Increasingly, studies have reported the neuroprotective effects of minocycline in neurologic diseases, such as ischemic stroke, multiple sclerosis, and traumatic brain injury (Fagan et al. 2011; Haber et al. 2013; Hahn et al. 2016). We demonstrated that minocycline significantly improved cognitive function after germinal matrix hemorrhage in rat pups on postnatal day 7 (p7) (Tang et al. 2016). Several clinical studies demonstrated the safety and tolerance of minocycline in stroke patients (Fouda et al. 2017; Hess and Fagan 2010), but larger randomized clinical trials are required to evaluate its efficacy (Chang et al. 2017).

Address for reprint requests and other correspondence: H. Miao, Department of Neurosurgery, Shanghai General Hospital affiliated to Shanghai Jiaotong University, 650 Xinsongjiang Rd., Shanghai, 210620, China (e-mail: miaohongsheng1973@yeah.net).

Table 1. *Primers used for RT-PCR*

Gene	ID in PubMed	mRNA Number	Primer Sequences
TrkB	25054	NM_012731.2	(FP) TTTGTGGCTTACAAGGCGTTTC
			(RP) GGTGGCGGAAATGTCTCCTG
BDNF	24225	NM_001270630.1	(FP) GTGGAAGAAACCGTCTAGAGCA
			(RP) CACCTGGTGGAACTGGATGAA
CD16	304966	NM_019218.2	(FP) AACGGCACTGCTACTTACGG
			(RP) CGAGATGAGGCTTTTGTTATGG
Nestin	25491	NM_001308239.1	(FP) AGAGAAGCGCTGGAACAGAG
			(RP) AGGTGTCTGCAACCGAGAGT
Arginase 1	29221	NM_017134.3	(FP) GGGAAAAGCCAATGAACAGC
			(RP) CCAAATGACGCATAGGTCAGG
Doublecortin	84394	NM_053379.3	(FP) TCGTAGTTTTGATGCGTTGC
			(RP) GCTTTCCCCTTCTTCCAGTT
Tuj-1	287847	NM_001134498.2	(FP) AGCAGATGCTGGCCATTCAGAGTA
			(RP) TAAACTGCTCGGAGATGCGCTTGA
Gapdh	24383	NM_017008.4	(FP) AAGGGCTCATGACCACAGTC
			(RP) GTGAGCTTCCCATTCAGCTC

FP, forward primer; RP, reverse primer.

Several neuroprotective mechanisms were reported to be targets after stroke, including inhibition of Toll-like receptors (TLR2 and TLR4) for anti-inflammation, NF-κB inhibition for resistance of metabolic disease (Baker et al. 2011), and blockade of phosphoinositide 3-kinase (PI3K)/Akt pathway to alleviate LPS-induced neuroinflammation (Pang et al. 2012). Few mechanisms of neurogenesis promotion, except neurotrophic factors, are widely accepted. Neurotrophins [NGF, brain-derived neurotrophic factor (BDNF)] and their specific receptors, the Trk family of tyrosine kinase receptors (TrkA, TrkB, TrkC), play key roles in brain restoration after injury (Kaplan and Miller 2000; Patapoutian and Reichardt 2001). The TrkB/BDNF pathway is widely accepted as the key pathway in brain repair after injury (Gustafsson et al. 2003; Ploughman et al. 2009).

The present study investigated the effects of minocycline on neurogenesis after ICH and the role of M2 microglia-derived neurotrophic factors in the neuroprotective process.

MATERIALS AND METHODS

Reagents. Minocycline was purchased from Sigma-Aldrich (St. Louis, MO, catalog no. M9511). Several doses were studied previously in rats after stroke, and 45 mg/kg via an intraperitoneal injection (ip) was proven to be neuroprotective. The dose used in the current

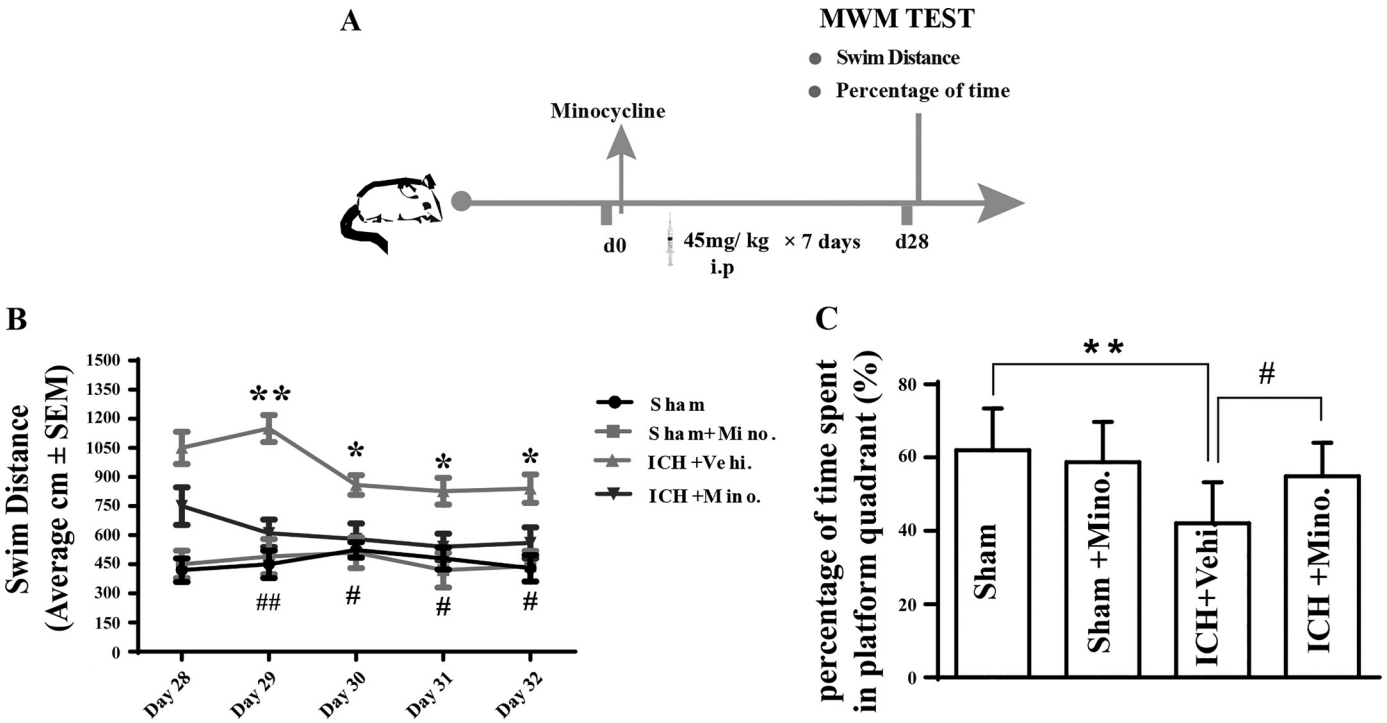

Fig. 1. Study protocol for minocycline administration and the time points for the behavioral and cognitive tests (*A*). Changes in the swimming distance of animals in the Morris water maze (MWM) from *day 28* (d28) to *day 32* after intracerebral hemorrhage (ICH; *B*). Rats spent less time in the targeted quadrants after ICH, and rats administered minocycline (Mino.) for 7 days spent more time in the targeted quadrant compared with rats in the vehicle (Vehi.)-treated group (*C*; $n = 12$). $^{*}P < 0.05$, $^{**}P < 0.01$, ICH + Vehi. vs. sham; $\#P < 0.05$, $\#\#P < 0.01$ indicate ICH + Mino. vs. ICH + Vehi. Two-way ANOVA with the Bonferroni post hoc test was used, and data are expressed as means ± SE.

study was previously reported (Zhao et al. 2011). *N*-[2-(5-hydroxy-1H-indol-3-yl) ethyl]-2-oxopiperidine-3-carboxamide (HIOC) is a derivative of *N*-acetyl serotonin that selectively activates the TrkB receptor. [N2–2-2-oxoazepan-3-yl amino] carbonyl phenyl benzo (b) thiophene-2-carboxamide (ANA 12) is a selective TrkB antagonist. Both drugs were purchased from Tocris Bioscience (catalog nos. 5961 and 4781) and injected intracerebroventricularly. Other reagents are mentioned in the text where appropriate.

Experimental ICH in rats and study protocol. A total of 150 Sprague-Dawley (S-D) rats (250–350 g, from the Third Military Medical University) were used in the study. All methods were performed in accordance with animal care guidelines at the Animal Ethics Committee of the Third Military Medical University, and the Southwest Hospital of the Third Military Medical University approved all experimental protocols [SYXK(Yu)2012-0012]. ICH in rats was induced via an injection of autologous blood from the femoral arteria as previously described (Jiang et al. 2017). Briefly, animals were placed on a feedback-controlled heating pad after anesthetization using pentobarbital (40 mg/kg ip). Animals were stereotaxically positioned, and a 1.0-mm-diameter cranial burr hole was drilled. A 29-gauge needle was inserted into the right caudate nucleus (coordinates: 0.2 mm anterior, 5.5 mm ventral and 3.5 mm lateral to the bregma). Each rat was injected with 100 μl of autologous arterial blood using a microinfusion pump at a constant rate of 10 μl/min. Arterial blood pressure, glucose level, Pa_{O_2} and Pa_{CO_2} were monitored during the procedure. Minocycline was injected ip 15 min after surgery and 12 h later. For long-term investigations, minocycline was injected twice daily for 7 days (ip). ANA 12 and HIOC were injected intracerebroventricularly 3 h after ICH.

Forty-six S-D rats were randomly divided into four groups (Sham, Sham + minocycline, ICH + vehicle, and ICH + minocycline) to

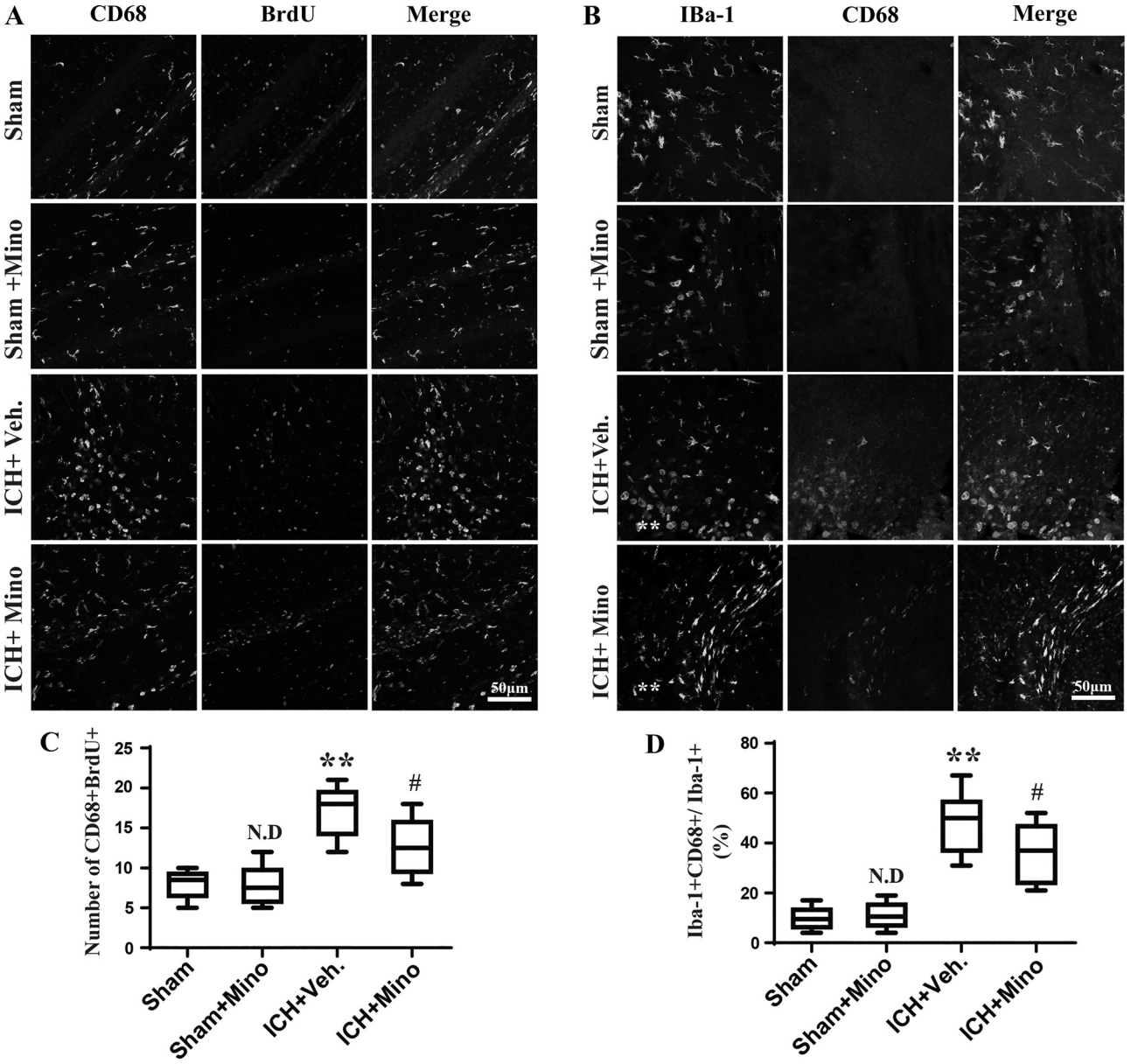

Fig. 2. Coexpression of M1-microglia marker protein (CD68) and BrdU in the brains of different groups (*A*). Coexpression of M1-microglia (CD68) and the general microglial marker Iba1 in four different groups (*B*). Statistical analyses of the number of CD68(+) BrdU(+) cells around the hematoma (*C*) and the percentage of CD68+ cells out of all Iba1-positive microglia (*D*). White double asterisks in *B* indicate the hematoma. $^{**}P < 0.01$ indicates intracerebral hemorrhage (ICH) + vehicle (Veh.) vs. sham, $\#P < 0.05$ indicates ICH + minocycline (Mino.) vs. ICH + Veh. Two-way ANOVA with the Bonferroni post hoc test was used, and data are expressed as means ± SE. N.D, not detected.

detect the long-term (28–32 days) effects of minocycline using behavior testing and magnetic resonance imaging (MRI) image changes. Six rats died during the ICH and MRI anesthesia procedure.

Twenty-four rats were used for immunohistochemistry detecting the effects of minocycline on microglial polarization, neurogenesis and TrkB/BDNF expression after ICH.

We randomly divided 80 rats into four groups: ICH + vehicle, ICH + minocycline, ICH + minocycline + ANA 12, and ICH + HIOC. Among them, in each group six rats were used for PCR detection, six for Western blot assays, and six for immunofluorescence. We lost eight rats during the procedure.

Intracerebroventricular injection. Intracerebroventricular injections were used For ANA 12 and HIOC administration as reported previously (Tang et al. 2015). Briefly, a small burr hole was drilled into the left skull relative to bregma: 1.5 mm posterior; 1.0 mm lateral. A 10-μl Hamilton syringe filled with ANA 12 (2 μg in 5 μl of DMSO) or HIOC (6 μg in 5 μl of DMSO) was stereotaxically inserted into the left lateral ventricle through the burr hole to a 4.0-mm depth. The microinjection rate was 0.5 μl/min.

Morris water maze test. All animals were subjected to a modified Morris water maze (MWM) test 28 days after ICH and drug administration (Ahn et al. 2013). Briefly, rats were placed in a metal pool (50 cm in depth, 200 cm in diameter) filled with water to find the submerged platform within 90 s. Each rat performed eight trials daily for 4 days, and the latency time was monitored and averaged across the trials. Acquisition training was performed over 5 days using a random set of start locations in the four quadrants. The animals were tested for spatial memory retention 24 h after the final trial. Visible platform trials were performed on *day 6* to assess visual acuity. The swim distance in the target quadrant and percentage of time spend in the quadrant where the platform used to be were calculated in the study ($n = 10$).

5-Bromo-2-deoxyuridine labeling. 5-Bromo-2-deoxyuridine (BrdU, Sigma) in 0.9% saline was administered (100 mg/kg ip twice daily for 3 days) as previously described with slight modifications (Lei et al. 2015).

Brain slice preparation and immunofluorescence. Rats were euthanized 3 days after ICH ($n = 6$). Frozen brain slices (18 μm) and immunofluorescence were performed as described previously (Tang et al. 2016). Slices were blocked with 5% bovine serum albumin and incubated overnight at 4°C with primary antibodies against BrdU (goat, Abcam, 1:500), Iba-1 (rabbit, WAKO, 1:1,000), MAP2 (mouse, Boster, 1:500), CD68 (mouse, AbD Serotec, 1:500), CD206 (mouse, Santa Cruz Biotechnology, 1:200), CD16 (mouse, Abcam, 1:500), and

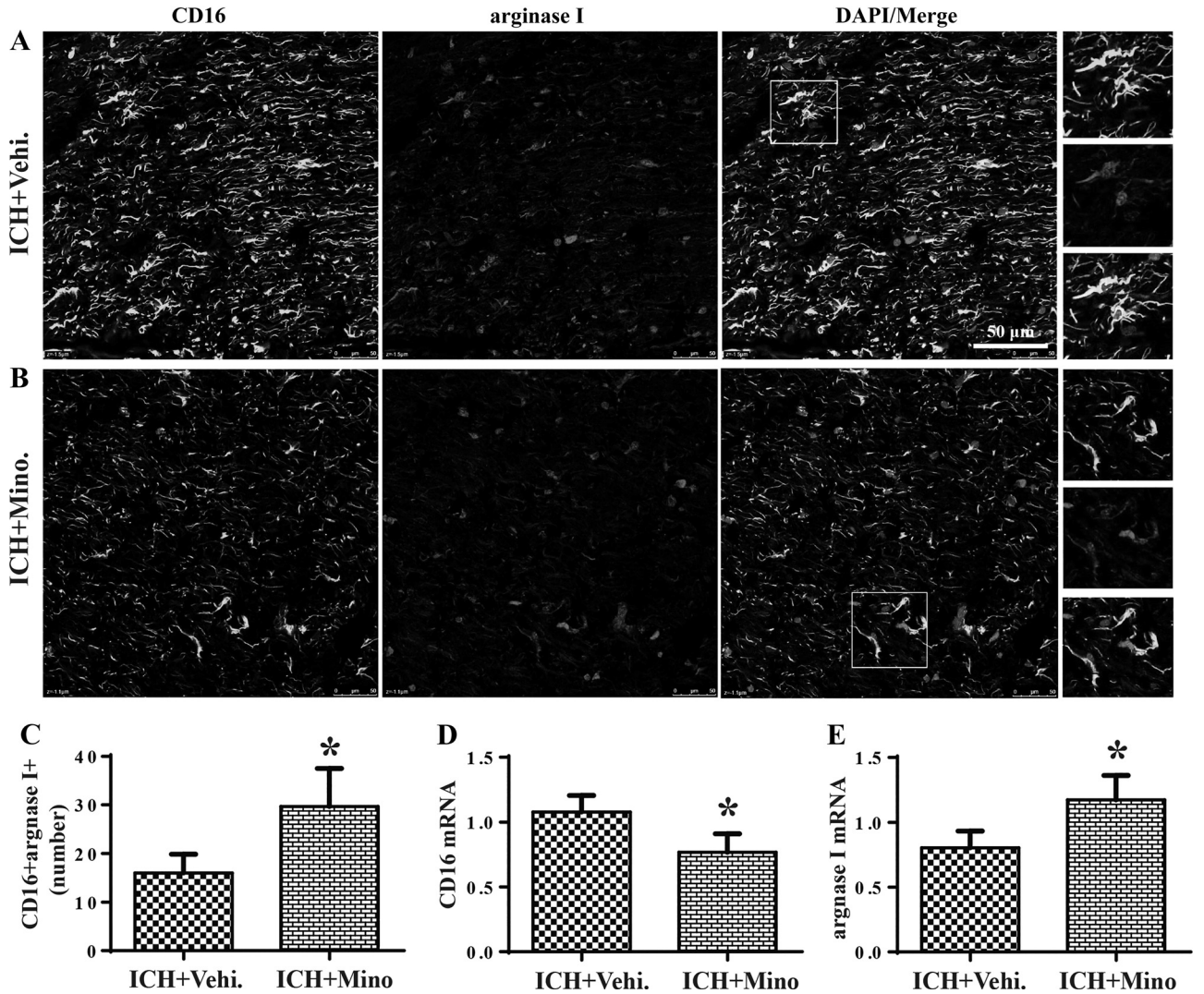

Fig. 3. Coexpression of the M1-microglia marker protein (CD16) and M2-microglia marker protein (arginase 1) in vehicle (Vehi.)-treated rats (*A*) and minocycline (Mino.)-treated rats (*B*). Statistical analyses of the number of CD16+ arginase 1+ cells in the two groups (*C*). RT-PCR analyses of the expression of CD16 mRNA (*D*) and arginase 1 mRNA (*E*) in rat brains treated with vehicle or minocycline. *$P < 0.05$. Data are expressed as means ± SE. ICH, intracerebral hemorrhage.

arginase 1 (rabbit, Santa Cruz Biotechnology, 1:200). Sections were washed and incubated with Alexa Fluor 488 (1:400, Abcam) or Cy3-labeled secondary antibodies (1:400, Jackson Laboratories) for 1 h at room temperature. DAPI (1:1,000, Beyotime Biotechnology) was used to stain cell nuclei. Images were captured using a ×20 or ×40 objective of a Zeiss confocal microscope (LSM780, Zeiss). Image J software was used to analyze the intensity of the regions of interest.

Western blot analysis. Western blotting was performed to measure the protein levels of MAP2, Tuj-1, DCX, nestin, NeuN, and TrkB in the brains of the animal groups ($n = 6$ for each group) as previously described (Chen et al. 2015). Rats were transcardially perfused with saline before decapitation, and ipsilateral coronary brain tissues (0–4 mm from the bregma) were collected on ice. Bicinchoninic acid protein concentration detection and SDS-PAGE were performed as previously reported (Jiang et al. 2017). The primary antibodies used were against TrkB (rabbit, Abcam, 1:1,000), MAP2 (mouse, Boster China, 1:500), Tuj-1 (mouse, Santa Cruz Biotechnology, 1:100), NeuN (rabbit, Abcam, 1:1,000), and nestin (mouse, Abcam, 1:1,000). GAPDH (diluted 1:1,000, Santa Cruz Biotechnology) was used as the loading control. Images were acquired using a ChemiDOCTMxrs+ system (Bio-Rad) and processed using Image Laboratory (Microsoft). Corresponding histograms were generated using GraphPad Prism 6 software.

Real-time PCR. Real-time PCR was used to detect changes in the mRNA levels of the TrkB pathway and NPCs (neural precursors cells), such as Tuj-1, DCX, and nestin, as described previously (Tao et al. 2016). Total RNA from the hematoma region was isolated using TRIzol reagent (Invitrogen, Carlsbad, CA). The primer sequences used were listed in Table 1. Expression levels were quantified with standard samples ($n = 6$).

Magnetic resonance imaging and cortical thickness measurement. A 7.0-T/200-mm Varian scanner (Bruker BioSpin) was used to calculate the thickness of the cortex after ICH and minocycline administration. MRI and the method for calculating cortical thickness were described previously (Tang et al. 2016). The T2 fast spin-echo sequence (TR/TE = 3,000/45 ms) was used for all animals after

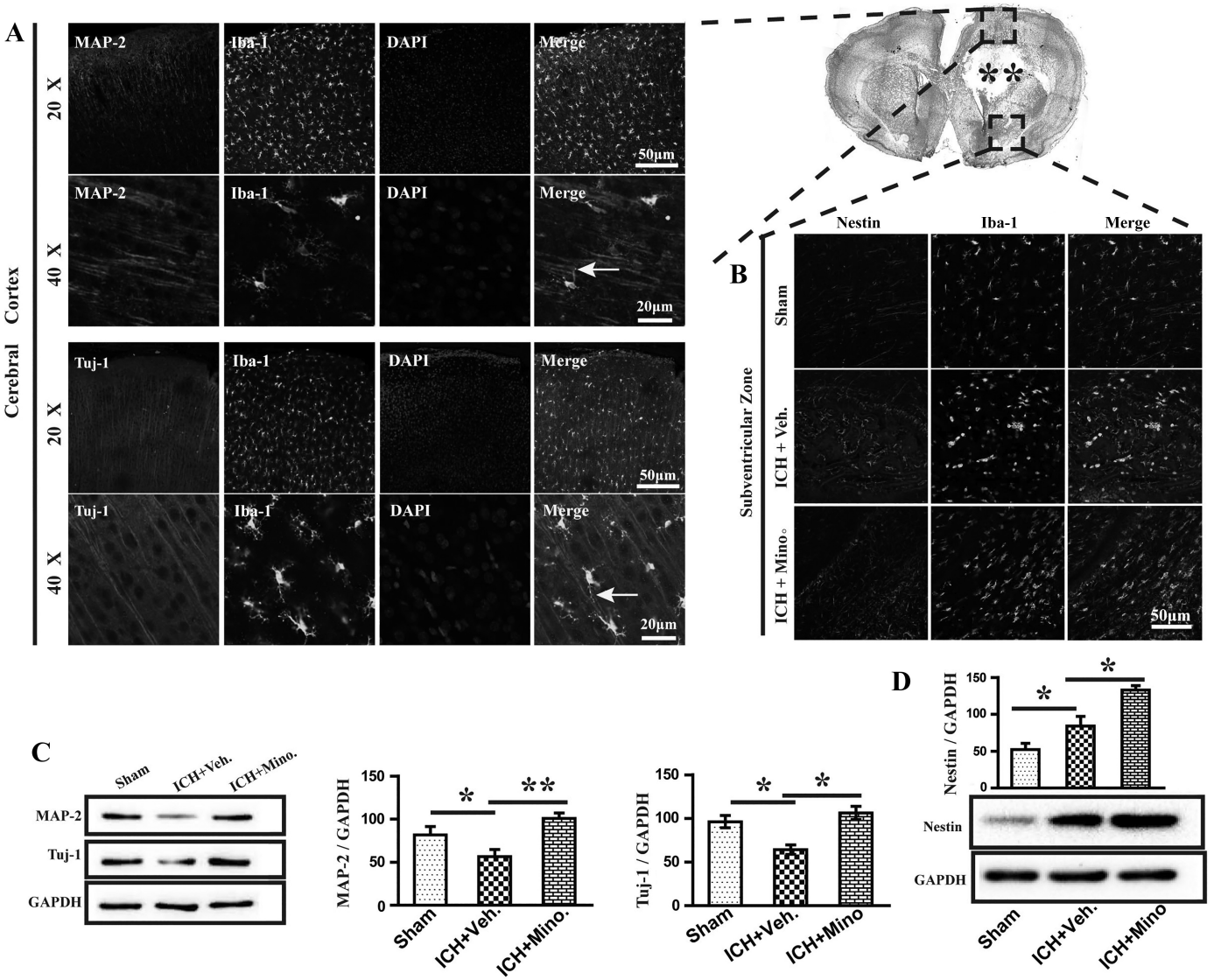

Fig. 4. Double-staining of MAP2 and microglia in the cortex at ×20 and ×40 and colabeling of Tuj-1 with microglia in the cortex (*A*). DAPI indicates the nucleus and arrows indicate the contact of microglia and neuronal dendrites. A hematoxylin and eosin slice is provided to indicate the sites of the specimen, and the black double asterisks indicate the hematoma. Coexpression of the NPC marker protein (nestin) and microglia (Iba1) in the subventricular zone (*B*). Images of Western blotting bands for MAP2 and Tuj-1 (*C*; $n = 6$), and statistical analyses using Image J in the sham, intracerebral hemorrhage (ICH) + vehicle (Veh.), and ICH + minocycline (Mino.) groups. Images of Western blotting bands and statistical analyses for nestin (*D*). $^*P < 0.05$, $^{**}P < 0.01$. Two-way ANOVA with Bonferroni post hoc test was used, and data are expressed as means ± SE.

behavioral testing. The field of view was 3.5×3.5 cm^2, and the matrix was 256×256. Seventeen coronal slices were obtained to cover the entire axis of the lateral ventricles (0.7 mm thick). Image J was used to measure the distance from the cingulum to layer II of the cortex in eight sections that were interspaced 0.7 mm and ranged from +3.2 to −3.8 from the bregma.

Golgi-Cox staining. Golgi-Cox staining was performed on brain tissue according to the protocol of the FD Rapid GolgiStain Kit (FD NeuroTechnologies).

Statistical analysis. All data are reported as means ± SE. The SPSS 13.0 software package (SPSS, Chicago, IL) was used for data analysis. One-way analysis of variance (ANOVA) was used as appropriate, followed by Student-Newman-Keuls tests. Two-way ANOVA with the Bonferroni post hoc test was used when necessary. A Welch's test was used in two-group comparisons. A P value less than 0.05 was considered statistically significant.

RESULTS

Minocycline improved long-term cognitive deficits after ICH. We designed an experimental protocol to measure the long-term cognitive effects (MWM test) 28 days after ICH and minocycline administration (Fig. 1*A*). ICH animals swam a significantly greater distance than those in the sham group in the MWM with the platform removed ($P < 0.01$, Fig. 1*B*). Minocycline-treated animals swam a significantly shorter distance than vehicle-injected animals. By contrast, minocycline administration to the sham group did not significantly impact learning memories in ICH rats. Rats in the ICH + vehicle group spent a shorter time in the targeted quadrant compared with rats in the ICH + minocycline group (Fig. 1*C*; $n = 12$).

Minocycline decreased the proliferation of M1 microglia and promoted M2 microglia polarization after ICH. We detected the proliferation and percentage of M1 microglia in the different groups to investigate the effects of minocycline on microglia polarization. We found a significant increase in CD68- and BrdU-positive cells around the hematoma in ICH brain tissue compared with sham animals ($P < 0.01$, Fig. 2, *A* and *C*). The number of CD68+ and BrdU+ cells decreased significantly after minocycline administration ($P < 0.05$, Fig. 2, *A* and *C*). ICH induced a higher percentage of CD68+ microglia than in the sham group ($P < 0.01$, Fig. 2, *B* and *D*). Fewer CD68-positive microglia around the hematoma were observed in minocycline-treated ICH brain slices compared with the vehicle-only group ($P < 0.05$, Fig. 2, *B* and *D*). No significant impact of minocycline on microglia was observed in sham animals.

We investigated the relationship between M1 and M2 microglia around the hematoma using immunohistochemistry and PCR after ICH and minocycline administration. Notably, a significant decrease in CD16-positive cells (M1 microglia) (Fig. 3*A*) and increase in CD16+ and arginase1+ cells (Fig. 3, *B* and *C*) was observed, which reflected the transformation of M1 microglia to M2 microglia after minocycline administration. Minocycline downregulated CD16 mRNA expression (Fig. 3*D*) after ICH and increased arginase 1 mRNA expression (Fig. 3*E*).

Minocycline enhanced microglia-synapse contacts in the cortex and induced neurogenesis. We measured the direct contacts of microglia and neuronal cells in the cortex (Fig. 4*A*) and examined the relationship between M2 microglia and nestin expression in the subventricular zone. More ramified microglia were found to be colabeled with nestin protein in minocycline-treated brain tissue than in vehicle-only brains (Fig. 4, *B* and *D*). ICH decreased the number of processes of neuronal cells and reduced MAP2 and Tuj-1 expression. Minocycline significantly increased the expression of these two proteins in neuronal processes (Fig. 4*C*). This self-restoration

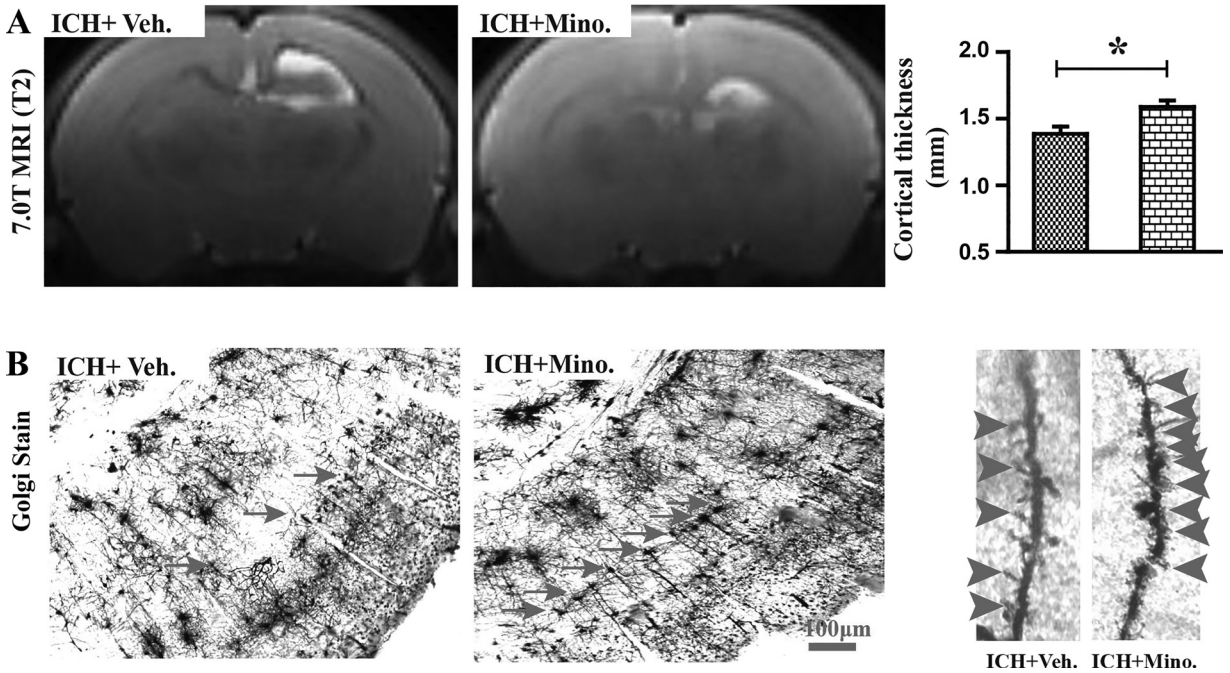

Fig. 5. Presentation of hematoxylin and eosin staining of brain slices in the intracerebral hemorrhage (ICH) + vehicle (Veh.) = and ICH + minocycline (Mino.) groups (*A*). 7.0 T2 MRI images of brains 28 days after ICH treatment with vehicle or minocycline and statistical analyses of the cortical thickness (*B*; $n = 10$). Slice of Golgi-Cox staining of an ICH brain treated with vehicle or minocycline and the magnified image of dendrites. Arrows indicate neurons and dendrites in the cortex, and the arrowheads indicate synapses on the dendrites (*C*; $n = 6$). *$P < 0.05$. Data are expressed as means ± SE.

increased the expression of some NPCs, such as nestin, and minocycline effectively enhanced ICH-induced self-restoration of neuronal cells.

We examined the effects of minocycline on the cerebral cortex and neuronal spinal dendrites and found a significant increase in the cerebral cortex thickness after minocycline treatment compared with vehicle-treated animals (Fig. 5*B*). Minocycline restored neuronal spinal dendrites after ICH and created more synapses (Fig. 5*C*).

Minocycline increased TrkB and BDNF expression in M2 microglia. Many ameboid microglia clustered around the hematoma after ICH. Minocycline transformed the ameboid microglia into ramified microglia with increased BDNF expression (Fig. 6*A*). PCR and Western blotting were used to measure TrkB expression. TrkB mRNA expression decreased 12 h after ICH and continued to decrease over the next 12 h to a stable level. Minocycline increased TrkB mRNA expression 6 h after ICH ($P < 0.05$, Fig. 6*B*). A significant decrease in TrkB protein expression was observed 24 h after ICH, and minocycline administration reversed this loss of TrkB ($P < 0.01$, Fig. 6*C*).

The TrkB/BDNF pathway played a pivotal role in minocycline-induced neurogenesis after ICH. Immunofluorescence and quantitative analyses revealed numerous changes: *1*) Minocycline reduced the ICH-induced increase in M1 polarized microglia (CD68+). A TrkB-selective antagonist reversed the effect of minocycline, and a TrkB-selective agonist produced similar effects on the number of CD68-positive cells (Fig. 7*A*). *2*) Minocycline and HIOC induced greater expression of M2-polarized microglia (CD206+) around the hematoma compared with vehicle-treated animals and animals treated with minocycline and ANA 12 (Fig. 7*B*). 3) Minocycline increased the number of mature neurons (NeuN+) in ICH animals, and ANA 12 reversed this neuroprotective effect (Fig. 7*C*). Integrated density analysis in the region of interest generated the same results (Fig. 7*D*).

We detected protein and mRNA expression of mature neurons (NeuN) and NPCs, such as Tuj-1, DCX, and nestin. Minocycline increased the expression of NeuN protein, which was reversed by ANA 12, and HIOC increased mature neuron expression to the same degree as minocycline (Fig. 8*A*). Minocycline increased the expression of Tuj-1, DCX, and nestin (Fig. 8, *B* and *C*) protein and mRNA. Selective blockade of the TrkB pathway automatically reversed the increase in NPC expression, and a TrkB agonist produced the same neuroprotective effects as minocycline.

DISCUSSION

The present study demonstrated that minocycline promoted neurogenesis and improved ICH-induced cognitive deficits after ICH. Minocycline produced neuroprotective effects via polarization of M2 neurotrophic microglia via the TrkB/BDNF pathway. ICH remains a significant medical emergency and requires a precise diagnosis as well as proper medical management (Hemphill et al. 2015). Minocycline was recently re-

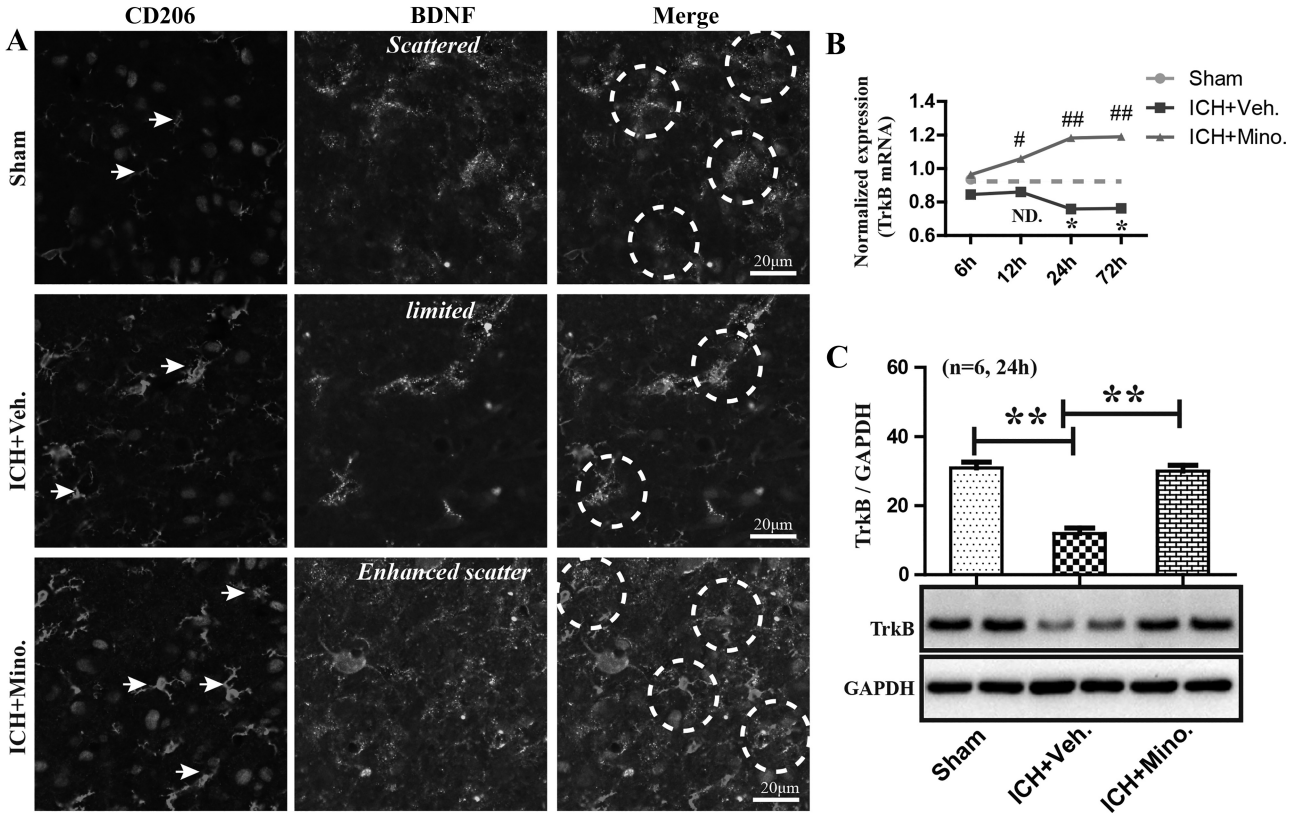

Fig. 6. Coexpression of M2-microglia (CD206) and brain-derived neurotrophic factor (BDNF) in the brains of different groups (*A*). White arrowheads indicate M2 microglia. White dashed circles indicate the location of contact between microglia, BDNF, and neurons. RT-PCR analysis of TrkB mRNA expression 6, 12, 24, and 72 h after ICH (*B*). Image of Western blotting bands and statistical analyses of TrkB protein expression 24 h after ICH (*C*; $n = 6$). ND, not detected. *$P < 0.05$, intracerebral hemorrhage (ICH) + vehicle (Veh.) vs. sham; #$P < 0.05$ ##$P < 0.01$, ICH + minocycline (Mino.) vs. ICH + Veh. Data are expressed as means ± SE.

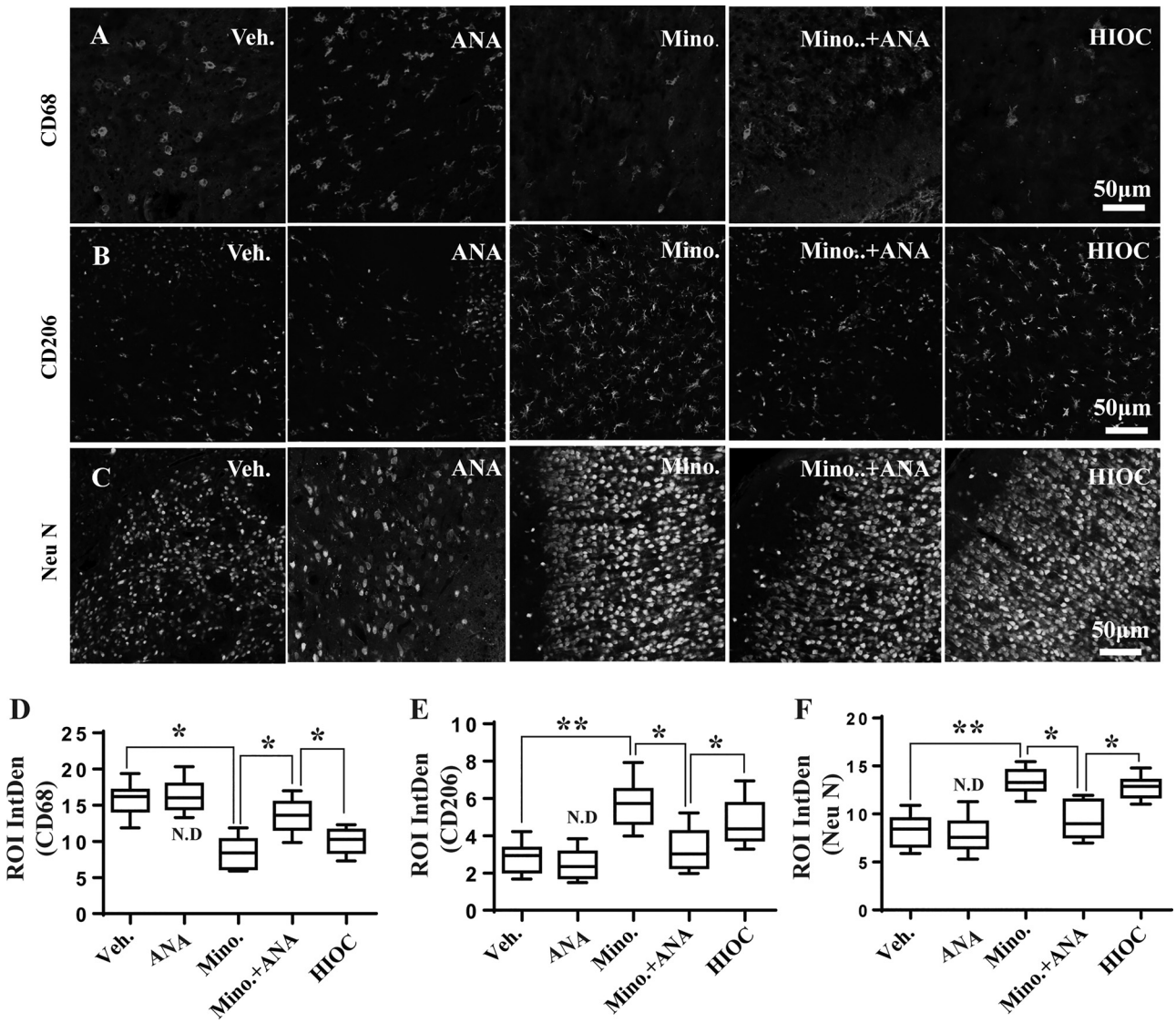

Fig. 7. Immunofluorescence of CD68-positive microglia in intracerebral hemorrhage (ICH) animals treated with vehicle, minocycline, or minocycline (Mino.) and N2–2-2-oxoazepan-3-yl amino] carbonyl phenyl benzo (b) thiophene-2-carboxamide (ANA 12; ANA), and animals treated with *N*-[2-(5-hydroxy-1H-indol-3-yl) ethyl]-2-oxopiperidine-3-carboxamide (HIOC) only (*A*). Images of CD206-positive microglia in brain slices of the four different groups (*B*). Immunofluorescence of mature neurons (*C*; NeuN+). Statistical analyses of the integrated density (IntDen) of positive cells in the regions of interest (ROI) in the brain slices of animals in different groups (*D*; $n = 6$). $^{*}P < 0.05$, $^{**}P < 0.01$. Data are expressed as means ± SE.

ported to be a potential pharmacological prevention strategy after stroke (Chang et al. 2017), but the effective targets and molecular mechanisms of minocycline are not known (Soliman et al. 2015). The autologous blood-induced ICH model in rats is a reasonable and efficient method to mimic the pathological process of clinical ICH (Dang et al. 2017). We found that a 7-day administration of minocycline improved the learning and working memory of autologous blood-induced ICH rats. We demonstrated that minocycline activated microglia transformation to an M2 neurotrophic type and did not simply inhibit microglia proliferation. We demonstrated that minocycline accelerated M2 microglia secretion of neurotrophic factors via the TrkB/BNDF pathway, which promoted neurogenesis after ICH.

Activation of microglia after ICH produces detrimental consequences because activated microglia are implicated in central nervous system (CNS) autoimmune diseases via the secretion of inflammatory factors and antigen presentation (Cash et al. 1993). However, a switch from M1- to M2-microglia associated gene expression was reported (Deonarine et al. 2007). Therefore, the focus of microglia research focused on neuroprotective effects (Zhao et al. 2015). Many studies have reported that M2 microglia secrete anti-inflammatory cytokines and growth factors, which promote neurogenesis and remyelination following CNS injury (Edwards et al. 2006; Miron et al. 2013). The present study found that minocycline easily penetrated the BBB and decreased ICH-induced M1 microglia (CD68+) proliferation as well as the percentage of CD68-positive microglia. We used another M1 microglia marker protein (CD16) and M2 microglia marker protein (arginase 1) to investigate our hypothesis and found that minocycline increased the number of arginase 1+ CD16+ cells, which demonstrated that minocycline promoted the transformation of M1 microglia into an M2 type after ICH in rats. Minocycline

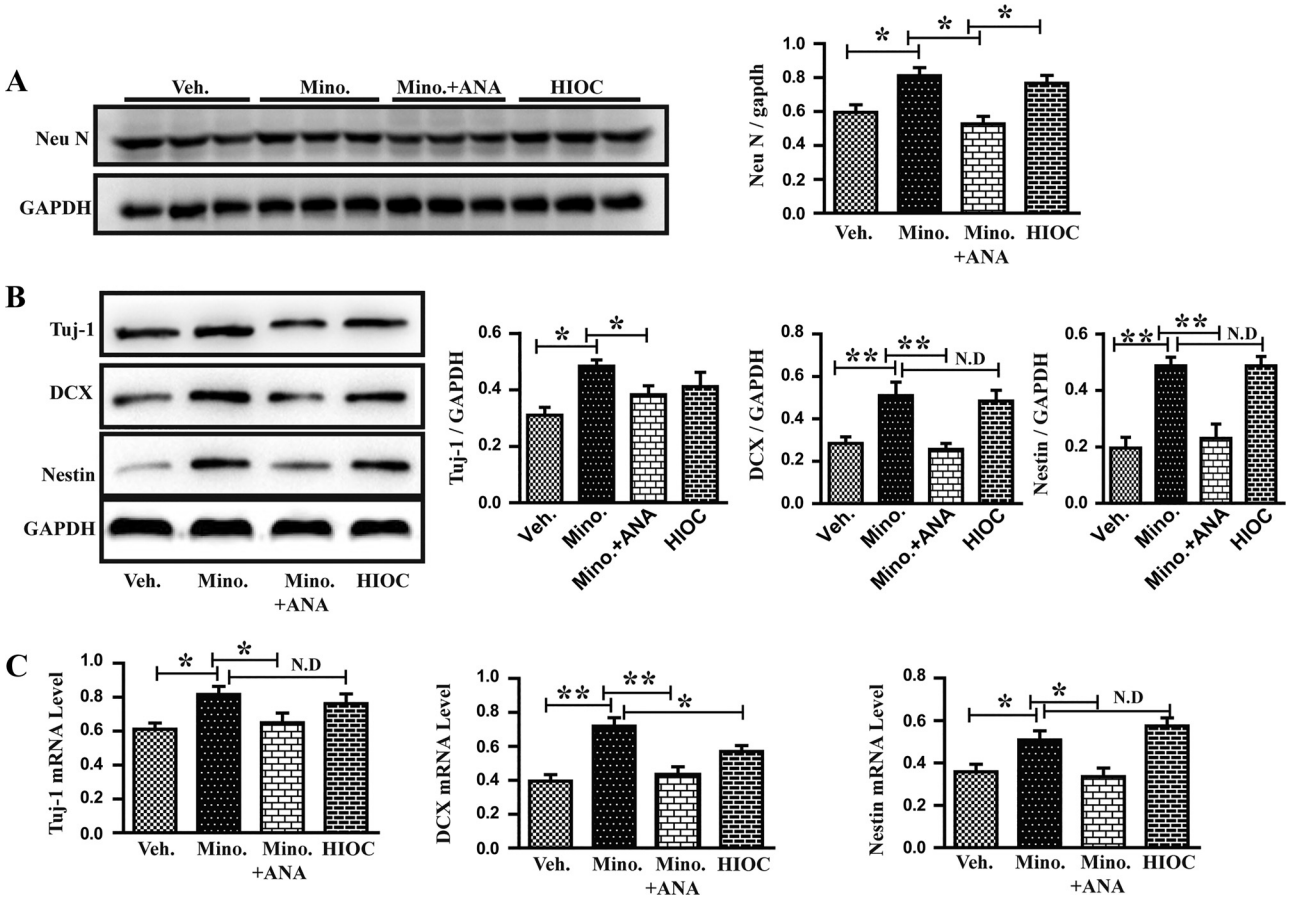

Fig. 8. Presentation of Western blotting bands and statistical analyses of NeuN protein expression in intracerebral hemorrhage (ICH) brain tissue treated with vehicle, minocycline, minocycline and N2–2-2-oxoazepan-3-yl amino] carbonyl phenyl benzo (b) thiophene-2-carboxamide (ANA 12) and animals treated with *N*-[2-(5-hydroxy-1H-indol-3-yl) ethyl]-2-oxopiperidine-3-carboxamide (HIOC) only (*A*). Presentation of Western blotting bands and statistical analyses of Tuj-1, DCX, and nestin in brain tissues from animals in different groups (*B*; $n = 6$). RT-PCR analyses of Tuj-1, DCX, and nestin in ICH brain tissues 24 h after the administration of vehicle, minocycline, minocycline and ANA 12, and HIOC only (*C*; $n = 6$). $^{*}P < 0.05$, $^{**}P < 0.01$. Data are expressed as means ± SE.

significantly increased the expression of M2 microglia-derived BDNF around neuronal cells, which suggests a role for BDNF and other neurotrophic factors in the restoration of neural circuits after ICH. A recent study demonstrated that microglial-derived BDNF increased neuronal TrkB phosphorylation, which is a key mediator of synaptic plasticity (Parkhurst et al. 2013).

The effects of minocycline are too complicated to be explained by a single mechanism. Several studies reported the positive effects of minocycline in improving cognitive damages in CNS diseases by inhibiting microglia or astrocytes activation (Cai et al. 2010; Hanlon et al. 2016). An in vitro study demonstrated that minocycline reduced the number of macrophages and decreased neuron death (Huang et al. 2010). Minocycline may inhibit MMP-9 and modulate BBB permeability as well as affect secondary injury of ICH (Shi et al. 2011). Minocycline also causes widespread cell death and increases the number of Iba1-positive microglia in neonatal mouse brain (Strahan et al. 2017). The present study demonstrated that minocycline induced greater expression of marker proteins of NPCs, such as DCX, Tuj-1, and nestin, and promoted the expression of mature neurons. The TrkB-selective antagonist ANA 12 reversed the protective effects of minocycline (i.e., decrease in M1 microglia and NPC proliferation), and the TrkB selective agonist HIOC produced similar neuroprotective effects as minocycline. A previous study used a systems biology approach and demonstrated that minocycline efficiently stimulated the TrkB/BDNF pathway (Alam et al. 2016).

Minocycline has been used clinically as an antibacterial medicine, but it is still being studied preclinically for the treatment of neuropathological disease. The present study demonstrated that minocycline improved ICH-induced learning and working memory deficits and promoted neurogenesis in rats. We demonstrated that the TrkB/BDNF pathway was partially involved in the protective effects of minocycline. The present study provides a novel understanding of the mechanisms with which minocycline could be useful in the treatment of ICH.

ACKNOWLEDGMENTS

The authors thank the Center of Teaching Experiments and College of Basic Medical Sciences of the Third Military Medical University for equipment assistance.

GRANTS

This work was supported by the National Science Foundation of China (NSFC, no. 81601356).

DISCLOSURES

No conflicts of interest, financial or otherwise, are declared by the authors.

AUTHOR CONTRIBUTIONS

M.H. conceived and designed research; M.H., R.L., C.H., X.L., and H.Z. performed experiments; M.H., X.L., and H.Z. analyzed data; M.H., R.L., C.H., and X.L. prepared figures; M.H. and C.H. drafted manuscript; M.H. approved final version of manuscript; R.L. interpreted results of experiments.

REFERENCES

Ahn SY, Chang YS, Sung DK, Sung SI, Yoo HS, Lee JH, Oh WI, Park WS. Mesenchymal stem cells prevent hydrocephalus after severe intraventricular hemorrhage. *Stroke* 44: 497–504, 2013. doi:10.1161/STROKEAHA.112.679092.

Alam MA, Subramanyam Rallabandi VP, Roy PK. Systems biology of immunomodulation for post-stroke neuroplasticity: multimodal implications of pharmacotherapy and neurorehabilitation. *Front Neurol* 7: 94, 2016. doi:10.3389/fneur.2016.00094.

Baker RG, Hayden MS, Ghosh S. NF-κB, inflammation, and metabolic disease. *Cell Metab* 13: 11–22, 2011. doi:10.1016/j.cmet.2010.12.008.

Cai ZY, Yan Y, Chen R. Minocycline reduces astrocytic reactivation and neuroinflammation in the hippocampus of a vascular cognitive impairment rat model. *Neurosci Bull* 26: 28–36, 2010. doi:10.1007/s12264-010-0818-2.

Cash E, Zhang Y, Rott O. Microglia present myelin antigens to T cells after phagocytosis of oligodendrocytes. *Cell Immunol* 147: 129–138, 1993. doi:10.1006/cimm.1993.1053.

Chang JJ, Kim-Tenser M, Emanuel BA, Jones GM, Chapple K, Alikhani A, Sanossian N, Mack WJ, Tsivgoulis G, Alexandrov AV, Pourmotabbed T. Minocycline and matrix metalloproteinase inhibition in acute intracerebral hemorrhage: a pilot study. *Eur J Neurol* 24: 1384–1391, 2017. doi:10.1111/ene.13403.

Chen Q, Tang J, Tan L, Guo J, Tao Y, Li L, Chen Y, Liu X, Zhang JH, Chen Z, Feng H. Intracerebral hematoma contributes to hydrocephalus after intraventricular hemorrhage via aggravating iron accumulation. *Stroke* 46: 2902–2908, 2015. doi:10.1161/STROKEAHA.115.009713.

Daly LT, Tsai DM, Singh M, Nuutila K, Minasian RA, Lee CC, Kiwanuka E, Hackl F, Onderdonk AB, Junker JP, Eriksson E, Caterson EJ. Topical minocycline effectively decontaminates and reduces inflammation in infected porcine wounds. *Plast Reconstr Surg* 138: 856e–868e, 2016. doi:10.1097/PRS.0000000000002633.

Dang G, Yang Y, Wu G, Hua Y, Keep RF, Xi G. Early erythrolysis in the hematoma after experimental intracerebral hemorrhage. *Transl Stroke Res* 8: 174–182, 2017. doi:10.1007/s12975-016-0505-3.

Deonarine K, Panelli MC, Stashower ME, Jin P, Smith K, Slade HB, Norwood C, Wang E, Marincola FM, Stroncek DF. Gene expression profiling of cutaneous wound healing. *J Transl Med* 5: 11, 2007. doi:10.1186/1479-5876-5-11.

Edwards JP, Zhang X, Frauwirth KA, Mosser DM. Biochemical and functional characterization of three activated macrophage populations. *J Leukoc Biol* 80: 1298–1307, 2006. doi:10.1189/jlb.0406249.

Fagan SC, Cronic LE, Hess DC. Minocycline development for acute ischemic stroke. *Transl Stroke Res* 2: 202–208, 2011. doi:10.1007/s12975-011-0072-6.

Fouda AY, Newsome AS, Spellicy S, Waller JL, Zhi W, Hess DC, Ergul A, Edwards DJ, Fagan SC, Switzer JA. Minocycline in acute cerebral hemorrhage: an early phase randomized trial. *Stroke* 48: 2885–2887, 2017. doi:10.1161/STROKEAHA.117.018658.

Gemma C, Bachstetter AD. The role of microglia in adult hippocampal neurogenesis. *Front Cell Neurosci* 7: 229, 2013. doi:10.3389/fncel.2013.00229.

Gustafsson E, Lindvall O, Kokaia Z. Intraventricular infusion of TrkB-Fc fusion protein promotes ischemia-induced neurogenesis in adult rat dentate gyrus. *Stroke* 34: 2710–2715, 2003. doi:10.1161/01.STR.0000096025.35225.36.

Haber M, Abdel Baki SG, Grin'kina NM, Irizarry R, Ershova A, Orsi S, Grill RJ, Dash P, Bergold PJ. Minocycline plus N-acetylcysteine synergize to modulate inflammation and prevent cognitive and memory deficits in a rat model of mild traumatic brain injury. *Exp Neurol* 249: 169–177, 2013. doi:10.1016/j.expneurol.2013.09.002.

Hahn JN, Kaushik DK, Mishra MK, Wang J, Silva C, Yong VW. Impact of minocycline on extracellular matrix metalloproteinase inducer, a factor implicated in multiple sclerosis immunopathogenesis. *J Immunol* 197: 3850–3860, 2016. doi:10.4049/jimmunol.1600436.

Hankey GJ. Stroke. *Lancet* 389: 641–654, 2017. doi:10.1016/S0140-6736(16)30962-X.

Hanlon LA, Huh JW, Raghupathi R. Minocycline transiently reduces microglia/macrophage activation but exacerbates cognitive deficits following repetitive traumatic brain injury in the neonatal rat. *J Neuropathol Exp Neurol* 75: 214–226, 2016. doi:10.1093/jnen/nlv021.

Hemphill JC III, Greenberg SM, Anderson CS, Becker K, Bendok BR, Cushman M, Fung GL, Goldstein JN, Macdonald RL, Mitchell PH, Scott PA, Selim MH, Woo D; American Heart Association Stroke Council; Council on Cardiovascular and Stroke Nursing; Council on Clinical Cardiology. Guidelines for the management of spontaneous intracerebral hemorrhage: a guideline for healthcare professionals from the American Heart Association/American Stroke Association. *Stroke* 46: 2032–2060, 2015. doi:10.1161/STR.0000000000000069.

Hess DC, Fagan SC. Repurposing an old drug to improve the use and safety of tissue plasminogen activator for acute ischemic stroke: minocycline. *Rev Neurol Dis* 7, *Suppl* 1: S7–S13, 2010.

Hu X, Leak RK, Shi Y, Suenaga J, Gao Y, Zheng P, Chen J. Microglial and macrophage polarization—new prospects for brain repair. *Nat Rev Neurol* 11: 56–64, 2015. doi:10.1038/nrneurol.2014.207.

Huang WC, Qiao Y, Xu L, Kacimi R, Sun X, Giffard RG, Yenari MA. Direct protection of cultured neurons from ischemia-like injury by minocycline. *Anat Cell Biol* 43: 325–331, 2010. doi:10.5115/acb.2010.43.4.325.

Jiang B, Li L, Chen Q, Tao Y, Yang L, Zhang B, Zhang JH, Feng H, Chen Z, Tang J, Zhu G. Role of glibenclamide in brain injury after intracerebral hemorrhage. *Transl Stroke Res* 8: 183–193, 2017. doi:10.1007/s12975-016-0506-2.

Kaplan DR, Miller FD. Neurotrophin signal transduction in the nervous system. *Curr Opin Neurobiol* 10: 381–391, 2000. doi:10.1016/S0959-4388(00)00092-1.

Kigerl KA, Gensel JC, Ankeny DP, Alexander JK, Donnelly DJ, Popovich PG. Identification of two distinct macrophage subsets with divergent effects causing either neurotoxicity or regeneration in the injured mouse spinal cord. *J Neurosci* 29: 13435–13444, 2009. doi:10.1523/JNEUROSCI.3257-09.2009.

Kim KH, Son SM, Mook-Jung I. Contributions of microglia to structural synaptic plasticity. *J Exp Neurosci* 7: 85–91, 2013. doi:10.4137/JEN.S11269.

Kobayashi K, Imagama S, Ohgomori T, Hirano K, Uchimura K, Sakamoto K, Hirakawa A, Takeuchi H, Suzumura A, Ishiguro N, Kadomatsu K. Minocycline selectively inhibits M1 polarization of microglia. *Cell Death Dis* 4: e525, 2013. doi:10.1038/cddis.2013.54.

Kumar A, Barrett JP, Alvarez-Croda DM, Stoica BA, Faden AI, Loane DJ. NOX2 drives M1-like microglial/macrophage activation and neurodegeneration following experimental traumatic brain injury. *Brain Behav Immun* 58: 291–309, 2016. doi:10.1016/j.bbi.2016.07.158.

Lan X, Han X, Li Q, Li Q, Gao Y, Cheng T, Wan J, Zhu W, Wang J. Pinocembrin protects hemorrhagic brain primarily by inhibiting toll-like receptor 4 and reducing M1 phenotype microglia. *Brain Behav Immun* 61: 326–339, 2017. doi:10.1016/j.bbi.2016.12.012.

Lei C, Wu B, Cao T, Zhang S, Liu M. Activation of the high-mobility group box 1 protein-receptor for advanced glycation end-products signaling pathway in rats during neurogenesis after intracerebral hemorrhage. *Stroke* 46: 500–506, 2015. doi:10.1161/STROKEAHA.114.006825.

Li L, Tao Y, Tang J, Chen Q, Yang Y, Feng Z, Chen Y, Yang L, Yang Y, Zhu G, Feng H, Chen Z. A cannabinoid receptor 2 agonist prevents thrombin-induced blood-brain barrier damage via the inhibition of microglial activation and matrix metalloproteinase expression in rats. *Transl Stroke Res* 6: 467–477, 2015. doi:10.1007/s12975-015-0425-7.

Miron VE, Boyd A, Zhao JW, Yuen TJ, Ruckh JM, Shadrach JL, van Wijngaarden P, Wagers AJ, Williams A, Franklin RJM, Ffrench-Constant C. M2 microglia and macrophages drive oligodendrocyte differentiation during CNS remyelination. *Nat Neurosci* 16: 1211–1218, 2013. doi:10.1038/nn.3469.

Pan J, Jin JL, Ge HM, Yin KL, Chen X, Han LJ, Chen Y, Qian L, Li XX, Xu Y. Malibatol A regulates microglia M1/M2 polarization in experimental stroke in a PPARγ-dependent manner. *J Neuroinflammation* 12: 51, 2015. doi:10.1186/s12974-015-0270-3.

Pang T, Wang J, Benicky J, Saavedra JM. Minocycline ameliorates LPS-induced inflammation in human monocytes by novel mechanisms including LOX-1, Nur77 and LITAF inhibition. *Biochim Biophys Acta* 1820: 503–510, 2012. doi:10.1016/j.bbagen.2012.01.011.

Parkhurst CN, Yang G, Ninan I, Savas JN, Yates JR III, Lafaille JJ, Hempstead BL, Littman DR, Gan WB. Microglia promote learning-dependent synapse formation through brain-derived neurotrophic factor. *Cell* 155: 1596–1609, 2013. doi:10.1016/j.cell.2013.11.030.

Patapoutian A, Reichardt LF. Trk receptors: mediators of neurotrophin action. *Curr Opin Neurobiol* 11: 272–280, 2001. doi:10.1016/S0959-4388(00)00208-7.

Perego C, Fumagalli S, Zanier ER, Carlino E, Panini N, Erba E, De Simoni MG. Macrophages are essential for maintaining a M2 protective response early after ischemic brain injury. *Neurobiol Dis* 96: 284–293, 2016. doi:10.1016/j.nbd.2016.09.017.

Ploughman M, Windle V, MacLellan CL, White N, Doré JJ, Corbett D. Brain-derived neurotrophic factor contributes to recovery of skilled reaching after focal ischemia in rats. *Stroke* 40: 1490–1495, 2009. doi:10.1161/STROKEAHA.108.531806.

Ponomarev ED, Maresz K, Tan Y, Dittel BN. CNS-derived interleukin-4 is essential for the regulation of autoimmune inflammation and induces a state of alternative activation in microglial cells. *J Neurosci* 27: 10714–10721, 2007. doi:10.1523/JNEUROSCI.1922-07.2007.

Quirié A, Demougeot C, Bertrand N, Mossiat C, Garnier P, Marie C, Prigent-Tessier A. Effect of stroke on arginase expression and localization in the rat brain. *Eur J Neurosci* 37: 1193–1202, 2013. doi:10.1111/ejn.12111.

Shi W, Wang Z, Pu J, Wang R, Guo Z, Liu C, Sun J, Gao L, Zhou R. Changes of blood-brain barrier permeability following intracerebral hemorrhage and the therapeutic effect of minocycline in rats. *Acta Neurochir Suppl* 110, *Suppl*: 61–67, 2011.

Soliman S, Ishrat T, Fouda AY, Patel A, Pillai B, Fagan SC. Sequential therapy with minocycline and candesartan improves long-term recovery after experimental stroke. *Transl Stroke Res* 6: 309–322, 2015. doi:10.1007/s12975-015-0408-8.

Strahan JA, Walker WH II, Montgomery TR, Forger NG. Minocycline causes widespread cell death and increases microglial labeling in the neonatal mouse brain. *Dev Neurobiol* 77: 753–766, 2017. doi:10.1002/dneu.22457.

Tang J, Chen Q, Guo J, Yang L, Tao Y, Li L, Miao H, Feng H, Chen Z, Zhu G. Minocycline attenuates neonatal germinal-matrix-hemorrhage-induced neuroinflammation and brain edema by activating cannabinoid receptor 2. *Mol Neurobiol* 53: 1935–1948, 2016. doi:10.1007/s12035-015-9154-x.

Tang J, Hu Q, Chen Y, Liu F, Zheng Y, Tang J, Zhang J, Zhang JH. Neuroprotective role of an N-acetyl serotonin derivative via activation of tropomyosin-related kinase receptor B after subarachnoid hemorrhage in a rat model. *Neurobiol Dis* 78: 126–133, 2015. doi:10.1016/j.nbd.2015.01.009.

Tao Y, Li L, Jiang B, Feng Z, Yang L, Tang J, Chen Q, Zhang J, Tan Q, Feng H, Chen Z, Zhu G. Cannabinoid receptor-2 stimulation suppresses neuroinflammation by regulating microglial M1/M2 polarization through the cAMP/PKA pathway in an experimental GMH rat model. *Brain Behav Immun* 58: 118–129, 2016. doi:10.1016/j.bbi.2016.05.020.

Wan S, Cheng Y, Jin H, Guo D, Hua Y, Keep RF, Xi G. Microglia activation and polarization after intracerebral hemorrhage in mice: the role of protease-activated receptor-1. *Transl Stroke Res* 7: 478–487, 2016. doi:10.1007/s12975-016-0472-8.

Zhao F, Hua Y, He Y, Keep RF, Xi G. Minocycline-induced attenuation of iron overload and brain injury after experimental intracerebral hemorrhage. *Stroke* 42: 3587–3593, 2011. doi:10.1161/STROKEAHA.111.623926.

Zhao H, Garton T, Keep RF, Hua Y, Xi G. Microglia/macrophage polarization after experimental intracerebral hemorrhage. *Transl Stroke Res* 6: 407–409, 2015. doi:10.1007/s12975-015-0428-4.